International Journal of Thermal Sciences 49 (2010) 235–242

Contents lists available at ScienceDirect

International Journal of Thermal Sciences

journal homepage: www.elsevier.com/locate/ijts

Thermal wave effects on heat transfer enhancement in nanofluids suspensions

Johnathan J. Vadasz [a,*], Saneshan Govender [b]

[a] Department of Mechanical and Aeronautical Engineering, University of Pretoria, Lynnwood Road, Pretoria 0002, South Africa
[b] Gas Division EED, ESKOM Arivia Business Park, Building 1, Simba Road, Sunninghill Johannesburg 2000, South Africa

ARTICLE INFO

Article history:
Received 10 March 2009
Received in revised form
20 May 2009
Accepted 3 June 2009

Keywords:
Nanofluids
Nanoparticles suspension
Heat transfer enhancement
Effective thermal conductivity

ABSTRACT

The heat transfer enhancement revealed experimentally in nanofluids suspensions is being investigated theoretically at the macro-scale level aiming at explaining the possible mechanisms that lead to such impressive experimental results. In particular, while the possibility that thermal wave effects via hyperbolic heat conduction could have explain the excessively improved effective thermal conductivity of the suspension the comparison with experimental results rules-out this explanation.

1. Introduction

A claimed effective thermal conductivity of up to a factor of 2.5 higher than that of the host-fluid was reported by Choi et al. [1] and by a factor of 1.4 by Eastman et al. [2]. While some of the more recent results question the validity of the latter and claim that these results were not replicated so far, the published evidence shows that if the experimental conditions were identical to the ones in the experimental setup of Choi et al. [1] and Eastman et al. [2] similar enhancement can be reached, e.g. Ref. [3]. All *relevant* experiments conducted by using the Transient Hot Wire method seem to reveal the same general trend of an impressive increase of the effective thermal conductivity of the suspension [2,1,4] far beyond the one predicted by using the effective medium theory [5–11]. In contrast, all experiments conducted by using optical methods [12–14] did not reveal such an enhancement and are perfectly consistent with the effective medium theory. The importance of discovering the correct mechanism and theory that underlies this phenomenon lies in the possibility to extend design options in developing processes and devices that apply these mechanisms, hence opening the door to yet unknown and limitless possibilities of new processes and devices that use heat transfer. Choi et al. [1] compared their results with exiting theories, some of them going back to the start of the last century, e.g. Refs. [5–11]. The reported experimental results are by one order of magnitude greater than the predictions based on existing theories and models. More recent approaches [16] also cannot explain this discrepancy.

There is a clear and appealing need to settle the conflict between the recent experimental results and the theories or models. Possible explanations for the divergence between theory and experiments were suggested and explored very basically by Brownian motion of the particles [17,18], micro-convection due to Brownian motion [19], molecular-level layering of the liquid at the liquid/particle interface [17,18,20], the nature of heat transport within the nanoparticles and effects of nanoparticle clustering [17,18], thermo-phoresis [21,22], electro-phoresis [21], hyperbolic heat conduction [23], Dual-phase-lagging effect of heat conduction in the nanofluid suspension [21]. To this end, most of these proposed mechanisms have been eliminated due to the theoretical outcomes of more detailed investigations except the dual-phase lagging, and that of nanoparticle clustering. The immediate conclusion from the latter deduction is that the Transient Hot Wire method (THW) that was used by Eastman et al. [2], Lee et al. [15] and by Choi et al. [1] to measure the nanofluid suspension's effective thermal conductivity is not appropriate because it uses the Fourier Law of heat conduction as its fundamental principle for estimating the thermal conductivity [24,25]. Eastman et al. [2] indicate the way the thermal conductivity is being evaluated by using Fourier Law in the Transient Hot Wire (THW) method. Therefore, based on this simple logic the excessive values of effective thermal conductivity calculated based on the

* Corresponding author.
E-mail addresses: johnathan.vadasz@up.ac.za (J.J. Vadasz), saneshan.govender@eskom.co.za (S. Govender).

1290-0729/$ – see front matter © 2009 Elsevier Masson SAS. All rights reserved.
doi:10.1016/j.ijthermalsci.2009.06.002

Nomenclature

Latin symbols

c^*	wave speed, equals $\sqrt{\alpha_*/\tau_*}$
Fo	Fourier number, equals $\alpha_*\tau_*/r_{o^*}^2$
i	electrical current
k^*	effective thermal conductivity of the suspension
l^*	length of the platinum wire/strip
$\boldsymbol{q}^*$	heat flux
$q_0{}^*$	horizontal heat flux on the boundary of the platinum wire, at $r^* = r_w{}^*$
$\dot{q}_{*l}$	rate of heat generated by Joule heating in the platinum wire per unit length of wire
R	electrical resistance, dimensional
r^*	radial variable co-ordinate
$r_w{}^*$	radius of the platinum wire
$r_0{}^*$	radius of the cylindrical container
t^*	time
T	dimensionless temperature, equals $(T^* - T_C{}^*)k^*/(q_o{}^* r_o{}^*)$
$T_C{}^*$	coldest wall temperature, dimensional
$T_1{}^*$	temperature measured at time $t^*{}_1$
$T_2{}^*$	temperature measured at time $t^*{}_2$
V	voltage across the platinum wire, dimensional
x	horizontal variable co-ordinate

Greek symbols

α^*	effective thermal diffusivity of the suspension
τ^*	relaxation time in hyperbolic thermal conduction

Subscripts

$*$	dimensional values
cr	critical values

experimental data might need a correction to account for deviations from Fourier Law.

The present paper demonstrates that while thermal wave effects via hyperbolic heat conduction [26–29] could have explain the excessively improved effective thermal conductivity of the suspension their comparison with experimental results [30] rule-out this explanation.

2. Experimental methods for thermal conductivity estimation

The Transient Hot Wire (THW) method for estimating experimentally the thermal conductivity of solids [31] and fluids [32–34] established itself as the most accurate, reliable and robust technique [35]. It replaced the steady state methods primarily because of the difficulty to determine that steady state conditions haven indeed been established and for fluids the difficulty in preventing the occurrence of natural convection and consequently the difficulty in eliminating the natural convection effects on the heat flux. The method consists in principle of determining the thermal conductivity of a selected material/fluid by observing the rate at which the temperature of a very thin platinum wire (5–80 μm) increases with time after a step change in voltage has been applied to it. The platinum wire is embedded vertically in the selected material/fluid and serves as a heat source as well as a thermometer, as presented schematically in Fig. 1. The temperature of the platinum wire is established by measuring its electrical resistance, the latter being related to the temperature via a well-known relationship. A Wheatstone bridge is used to measure the electrical resistance R_w of the platinum wire (see Fig. 1). The electrical resistance of the potentiometer R_3 is adjusted until the reading of the galvanometer G shows zero current. When the bridge is balanced as indicated by a zero current reading on the galvanometer G, the value of R_w can be established from the known electrical resistances R_1, R_2 and R_3 by using the balanced Wheatstone bridge relationship $R_w = R_1R_3/R_2$. Because of the very small diameter (micrometer size) and high thermal conductivity of the platinum wire the latter can be regarded as a line source in an otherwise infinite cylindrical medium. The rate of heat generated per unit length (l^*) of platinum wire is therefore $\dot{q}_{*1} = iV/l_*$ [W/m], where i is the electric current flowing through the wire and V is the voltage drop across the wire. Solving for the radial heat conduction due to this line heat source leads to a temperature solution in the following closed form that can be expanded in an infinite series as follows

$$T_* = \frac{\dot{q}_{*1}}{4\pi k_*} Ei\left(\frac{r_*^2}{4\alpha_* t_*}\right) = \frac{\dot{q}_{*1}}{4\pi k_*}\left[-\gamma + \ln\left(\frac{4\alpha_* t_*}{r_*^2}\right) + \frac{r_*^2}{4\alpha_* t_*} - \frac{r_*^4}{64\alpha_*^2 t_*^2} - \frac{r_*^6}{1152\alpha_*^3 t_*^3} - \cdots\right] \tag{1}$$

where $Ei(\cdot)$ represents the exponential integral function, and $\gamma = \ln(\sigma) = 0.5772156649$ is Euler's constant. For a line heat source embedded in a cylindrical cell of infinite radial extent and filled with the test fluid one can use the approximation $r_*^2/4\alpha_* t_* \ll 1$ in Eq. (1) to truncate the infinite series and yield

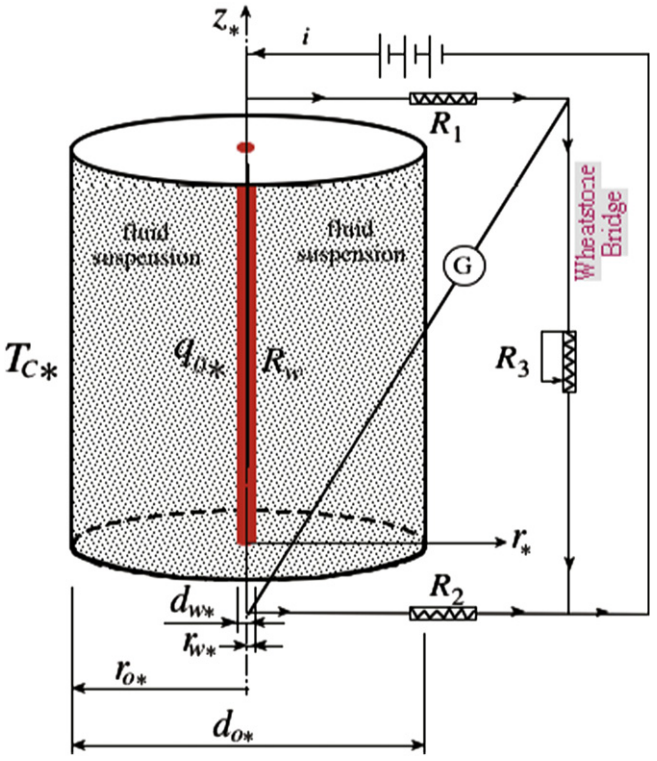

Fig. 1. Problem formulation of heat conduction in a cylindrical annulus subject to a combination of constant temperature (Dirichlet) and constant heat flux (Neumann) boundary conditions and the Transient Hot Wire configuration.

$$T_* \approx \frac{\dot{q}_{*1}}{4\pi k_*}\left[-\gamma + \ln\left(\frac{4\alpha_* t_*}{r_*^2}\right) + O\left(\frac{r_*^2}{4\alpha_* t_*}\right)\right] \quad (2)$$

Eq. (2) reveals a linear relationship, on a logarithmic time scale, between the temperature and time. For $r^* = r_{w^*}$, r_{w^*} being the radius of the platinum wire, the condition for the series truncation $r_*^2/4\alpha_* t_* \ll 1$ can be expressed in the following equivalent form that provides the validity condition of the approximation in the form

$$t_* \gg \frac{r_{w^*}^2}{4\alpha_*} \quad (3)$$

For any two temperature readings T_{1^*} and T_{2^*} recorded at the times t^*_1 and t^*_2 respectively the temperature difference $(T_{2^*} - T_{1^*})$ can be approximated by using Eq. (2) in the form

$$(T_{2^*} - T_{1^*}) \approx \frac{iV}{4\pi k_* l_*}\left[\ln\left(\frac{t_{*2}}{t_{*1}}\right)\right] \quad (4)$$

where we replaced the heat source with its explicit dependence on the i,V and l^*, i.e., $\dot{q}_{*1} = iV/l_*$. From Eq. (4) one can express the thermal conductivity k^* explicitly in the form

$$k_* \approx \frac{iV}{4\pi(T_{2^*} - T_{1^*})l_*}\left[\ln\left(\frac{t_{*2}}{t_{*1}}\right)\right] \quad (5)$$

Eq. (5) is a very accurate way of estimating the thermal conductivity as long as the validity conditions for appropriateness of problem derivations used above are fulfilled. A finite length of the platinum wire, the finite size of the cylindrical container, the heat capacity of the platinum wire, and possibly natural convection effects are examples of possible deviations of any realistic system from the one used in deriving Eq. (5). De Groot et al. [32], Healy et al. [33], and Kestin and Wakeham [34] introduce an assessment of these deviations and possible corrections to the THW readings to improve the accuracy of the results. In general all the deviations indicated above could be eliminated via the proposed corrections provided the validity condition listed in Eq. (3) is enforced as well as an additional condition that ensures that natural convection is absent. The validity condition (3) implies the application of Eq. (5) for long times only. However, when evaluating this condition (3) to data used in the nanofluids suspensions experiments considered in this paper one obtains explicitly the following values. For a 76.2 μm diameter of platinum wire used by Eastman et al. [2], Lee et al. [15], Choi et al. [1], the wire radius is $r_{w^*} = 3.81 \times 10^{-5}$ m leading to $r_{w^*}^2/4\alpha_* = 3.9$ ms for Ethylene Glycol and $r_{w^*}^2/4\alpha_* = 4.2$ ms for oil, leading to the validity condition $t_* \gg 3.9$ ms for Ethylene Glycol and $t_* \gg 4.2$ ms. The long times beyond which the solution (5) can be used reliably are therefore of the order of a tens of milliseconds, not so long in the actual practical sense. On the other hand the experimental time range is limited from above as well in order to ensure the lack of natural convection that develops at longer time scales. Xuan and Li [4] estimate this upper limit for the time that an experiment may last before natural convection develops as about 5 s. They indicate that "*An experiment lasts about 5 s. If the time is longer, the temperature difference between the hot-wire and the sample fluid increases and free convection takes place, which may result in errors*". Lee et al. [15] while using the THW method and providing experimental data in the time range of 1 s to 10 s, indicate in their Fig. 3 the "*valid range of data reduction*" to be between 3 s and 6 s. Our estimations evaluated above confirm these lower limits as a very safe constraint and we assume that the upper limits listed by Xuan and Li [4] and Lee et al. [15] are also good estimates, leading to the validity condition of the experimental results to be within the following estimated time range of $0.03\text{ s} < t^* < 6$ s. The valid range for data reduction used by Lee et al. [15], i.e., $3\text{ s} < t^* < 6$ s should also be satisfactory. Within this time range the experimental results should produce a linear relationship, on a logarithmic time scale, between the temperature and time.

While the application of the method to gases is straightforward its corresponding application to electrically conducting liquids and solids needs further attention. The experiments conducted in nanofluids suspensions listed above [1,2,4] used a thin electrical insulation coating layer to cover the platinum wire instead of using the bare metallic wire, a technique developed by Nagasaka and Nagashima [36]. The latter is aimed at preventing problems such as electrical current flow through the liquid causing ambiguity of the heat generation in the wire. In the case of solids Assael et al. [31,37–40] demonstrates the importance of using an intermediate soft solid material between the hot wire and the solid of interest in order to eliminate or substantially reduce contact thermal resistances. Therefore, the bare metallic wire can only be used for gases, e.g. de Groot et al. [41], or electrically insulating liquids such as oils.

Assael et al. [31,37–40] developed a new application of the Transient Hot Wire method by using a commercial software to solve the whole temperature-time curve by trial and error until it fits the experimental data, at which point the thermal conductivity (k) and the heat capacity (ρc_p) of the material are found. Assael et al. [31,37–40] showed the development of this method specifically for solids with only one example used for applying it to fluids, and without discussing the possible effects of convection on the latter. Preventing effects of convection in fluids is a particular emphasis that is substantially distinct from its application to solids. All these demonstrations still use experimental standards (e.g. diameter or cross sectional extent of the wire, length of the wire, wire material) that are within the validity range of the classical Transient Hot Wire method described above, although experimental results for time ranges of microseconds can be used when using the proposed method.

The impressive experimental results by Choi et al. [1] have not been confirmed nor reproduced so far. Assael et al. [42,43] attempted to confirm such results and showed an improved effective thermal conductivity of up to 38%, and the latter decays in time claimed to be due to homogenization. Although 38% improvement is substantially less than the 150% claimed by Choi et al. [1] it is still an impressive enhancement. Understanding the source of such discrepancies becomes an important task.

3. Problem formulation and thermal wave effects

The present investigation focuses on thermal wave effects via the constitutive model suggested by Cattaneo [26] and Vernotte [27–29] and the possible deviation of the experimental results due to these effects from the expected Fourier conduction. To investigate preliminary the possibility that thermal wave effects might have been the cause of the apparently spectacular enhancement of the effective thermal conductivity of the suspension we consider the thermal conduction in a cylindrical geometry due to the hot wire as the heat source (see Fig. 1) via the hyperbolic heat conduction formulation as well as via a Fourier heat conduction formulation and compare between the two. The cylindrical geometry used here applies to a Transient Hot Wire method of evaluation of the thermal conductivity and the comparison applies to deviations between Fourier to hyperbolic thermal conduction as applicable to the THW method and the required corrections in accounting for the latter deviations.

While the objective of this paper is to present the derivations of the solutions to the hyperbolic heat conduction problem the first step is to show the solution to the corresponding Fourier heat conduction. The reason for the latter is the need to have the

reference Fourier solution for comparison purposes as will be shown later. Consider the cylinder as described in Fig. 1 subject to a constant heat flux at $r_{w^*}q_{0^*}$, representing the heat flux from the hot wire to the fluid due to the uniform Joule heating generated in the thin hot wire by the electric current, and a constant cold temperature T_{C^*} at r_{0^*}. The Fourier conduction phenomenon is governed by the constitutive relationship between the heat flux and temperature gradient in the form

$$\boldsymbol{q}_* = -k_*\nabla_* T_* \tag{6}$$

and the energy balance equation

$$\rho_* c_{p^*}\frac{\partial T_*}{\partial t_*} = -\nabla_*\cdot\boldsymbol{q}_* \tag{7}$$

which lead to the Fourier heat conduction equation

$$\frac{\partial^2 T_*}{\partial r_*^2}+\frac{1}{r_*}\frac{\partial T_*}{\partial r_*}=\frac{1}{\alpha_*}\frac{\partial T_*}{\partial t_*} \tag{8}$$

where r^* is the independent variable in the radial direction and α^* is the thermal diffusivity. Eq. (8) may be transformed into a dimensionless form by introducing the following definitions of dimensionless variables

$$r=\frac{r_*}{r_{o^*}};\quad t=\frac{\alpha_* t_*}{r_{o^*}^2} \tag{9}$$

that transform Eq. (8) into its corresponding dimensionless form

$$\frac{\partial^2 T}{\partial r^2}+\frac{1}{r}\frac{\partial T}{\partial r}=\frac{\partial T}{\partial t} \tag{10a}$$

The boundary and initial conditions are expressed in the following dimensionless form

$$\begin{aligned} &r=r_w:\frac{\partial T}{\partial r}=-1\\ &r=1:T=0\end{aligned} \tag{11}$$

$$t=0:\begin{cases} T=T_o=\text{const.}\\ \dot{T}=\dot{T}_o=\text{const.}\end{cases} \tag{10b}$$

Eq. (10) has a steady state dimensionless solution as follows

$$T_s=-r_w\ln r \tag{12}$$

and a transient solution obtained via separation of variables in the form

$$T_t=\sum_{n=0}^{\infty}a_n e^{-\beta_n^2 t}R_{0n} \tag{13}$$

where a_n is represented by the following equation

$$a_n=\frac{I_1-I_2}{I_3} \tag{14}$$

and I_1, I_2, I_3 are definite integrals with the following solutions

$$I_1=\frac{T_0}{\beta_n}\left[\frac{2}{\pi\beta_n}-r_w R_0(\beta_n,r_w)\right] \tag{15a}$$

$$I_2=-\frac{r_w R_{0n}(\beta_n,r_w)}{\beta_n^2} \tag{15b}$$

$$I_3=N(\beta_n)=\frac{2}{\pi^2}\frac{J_0'2(\beta_n r_w)-J_0^2(\beta_n)}{\beta_n^2 J_0'2(\beta_n r_w)} \tag{15c}$$

where R_{0n} is represented by a linear combination of Bessel functions as follows

$$R_{0n}(\beta_n,r)=J_0(\beta_n r)Y_0(\beta_n)-J_0(\beta_n)Y_0(\beta_n r) \tag{16}$$

and β_n's are the positive roots of the following eigenvalues equation

$$J_0'(\beta_n r_w)Y_0(\beta_n)-J_0(\beta_n)Y_0'(\beta_n r_w)=0 \tag{17}$$

where J_0 and Y_0 are the order 0 Bessel functions of the first and second kind, respectively. Then, the complete Fourier solution (see Ref. [44] for details) has the form

$$T=T_s+T_t=-r_w\ln r+\sum_{n=0}^{\infty}\alpha_n e^{-\beta_n^2 t}R_{0n}(\beta n,r) \tag{18}$$

where a_n is defined by (14) and (15), R_{0n} by (16) and the β_n's are the roots obtained from solving Eq. (17).

The hyperbolic conduction phenomenon is governed by the constitutive relationship between the heat flux and temperature gradient in the form

$$\tau_*\frac{\partial \boldsymbol{q}_*}{\partial t_*}+\boldsymbol{q}_*=-k_*\nabla_* T_* \tag{19}$$

which combined with the energy balance Eq. (7) leads to the hyperbolic heat conduction equation

$$\frac{1}{c_*^2}\frac{\partial^2 T_*}{\partial t_*^2}+\frac{1}{\alpha_*}\frac{\partial T_*}{\partial t_*}=\nabla_*^2 T_* \tag{20}$$

where $c_*=\sqrt{\alpha_*/\tau_*}$ is the speed of wave propagation. Eqs. (19) and (20) may be transferred into a dimensionless form by introducing the following scales r_{0^*}, $r_{0^*}^2/\alpha^*$, q_{0^*}, $q_{0^*}L^*/k^*$ for the space variable, time variable, heat flux and temperature difference, respectively. This leads to the following definitions of the dimensionless variables

$$r=\frac{r_*}{r_{o^*}};\quad t=\frac{\alpha_* t_*}{r_{o^*}^2},\quad q=\frac{q_*}{q_{0^*}},\quad T=\frac{(T_*-T_{C^*})k_*}{q_{0^*}L_*} \tag{21}$$

that transform Eqs. (19) and (20) into their corresponding dimensionless form

$$Fo\frac{\partial \boldsymbol{q}}{\partial t}+\boldsymbol{q}=-\nabla T \tag{22}$$

$$Fo\frac{\partial^2 T}{\partial t^2}+\frac{\partial T}{\partial t}=\nabla^2 T \tag{23}$$

where $Fo=\alpha_*\tau_*/r_{0^*}^2$ is the Fourier number. For the one-dimensional slab considered here Eq. (23) takes the form

$$Fo\frac{\partial^2 T}{\partial t^2}+\frac{\partial T}{\partial t}=\frac{\partial^2 T}{\partial r^2}+\frac{1}{r}\frac{\partial T}{\partial r} \tag{24}$$

The boundary and initial conditions are expressed in the following dimensionless form

$$\begin{aligned} &r=r_w:\tfrac{\partial T}{\partial r}=-1\\ &r=1:T=0\end{aligned} \tag{25}$$

$$t=0:\begin{cases} T=T_0=\text{const.}\\ \dot{T}=\dot{T}_0=\text{const.}\end{cases} \tag{26}$$

Note that because the boundary heat flux at $r=r_w$ is constant, Eq. (22) with $(\partial q/\partial t)_{r=r_w}=0$, produces $(q_r)_{r=r_w}=-(\partial T/\partial r)_{r=r_w}$, a result that is identical to the Fourier boundary condition.

The solution to Eq. (24), subject to the boundary and initial conditions (25) and (26), obtained via separation of variables is expressed in terms of orthogonal eigenfunctions in the form

$$\begin{aligned} T &= T_s + T_t \\ &= -r_w \ln r + \sum_{n=1}^{n_{cr}-1} A_{n1}\left(e^{\lambda_1 t/Fo} - \lambda_{ND1} e^{\lambda_2 t/Fo}\right) R_0(\beta_n r) \\ &\quad + A_{n2} e^{\lambda t/Fo}(1 - \lambda t/Fo) R_0(\beta_{n_{cr}} r) \\ &\quad + \sum_{n_{cr}+1}^{\infty} A_{n_{cr}} e^{\lambda_1 t/Fo}[\cos(\lambda_{in} t/Fo) - \lambda_{ND2}\sin(\lambda_{in} t/Fo)] R_0(\beta_n r) \end{aligned} \tag{27}$$

where

$$\lambda_{1,2} = -\frac{1}{2}\left(1 \pm \sqrt{1 - 4Fo\beta^2}\right) \quad \forall \beta < \beta_{cr} \tag{28}$$

$$\lambda = -\frac{1}{2} \quad \forall \beta = \beta_{cr} \tag{29}$$

$$\lambda_r = -\frac{1}{2} \quad \forall \beta > \beta_{cr} \tag{30}$$

$$\lambda_{in} = \frac{1}{2}\left(\sqrt{4Fo\beta^2 - 1}\right) \quad \forall \beta > \beta_{cr} \tag{31}$$

$$\lambda_{ND1} = \frac{\lambda_1}{\lambda_2} \tag{32}$$

$$\lambda_{ND2} = \frac{\lambda_r}{\lambda_{in}} \tag{33}$$

$$A_{n1} = \frac{I_1 - I_2}{\left(1 - \frac{\lambda_1}{\lambda_2}\right) I_3} \quad \forall \beta < \beta_{cr} \tag{34a}$$

$$A_{n2} = A_{n_{cr}} = \frac{I_1 - I_2}{I_3} \quad \forall \beta = \beta_{cr} \tag{34b}$$

$$A_{n3} = A_{n2} = \frac{I_1 - I_2}{I_3} \quad \forall \beta > \beta_{cr} \tag{34c}$$

and I_1, I_2, I_3 are definite integrals with the following solutions

$$I_1 = \frac{T_0}{\beta_n}\left[\frac{2}{\pi\beta_n} - r_w R_0(\beta_n, r_w)\right] \tag{35a}$$

$$I_2 = -\frac{r_w R_{0n}(\beta_n, r_w)}{\beta_n^2} \tag{35b}$$

$$I_3 = N(\beta_n) = \frac{2}{\pi^2}\frac{J_0' 2(\beta_n r_w) - J_0^2(\beta_n)}{\beta_n^2 J_0' 2(\beta_n r_w)} \tag{35c}$$

where R_{0n} is represented by a linear combination of Bessel functions as follows

$$R_{0n}(\beta_n, r) = J_0(\beta_n r) Y_0(\beta_n) - J_0(\beta_n) Y_0(\beta_n r) \tag{36}$$

and β_n's are the positive roots of the following equation

$$J_0'(\beta_n r_w) Y_0(\beta_n) - J_0(\beta_n) Y_0'(\beta_n r_w) = 0 \tag{37}$$

where J_0 and Y_0 are the order 0 Bessel functions of the first and second kind, respectively. The value of β_{cr} can be expressed by equating the square root in Eq. (28) to zero, as follows

$$\beta_{cr} = \frac{1}{2\sqrt{Fo}} \tag{38}$$

The dimensionless distance between the wire and the cylinder wall is $(1 - r_w)$ and the dimensionless speed of wave propagation from Eq. (23) is $1/\sqrt{Fo}$, hence the dimensionless time needed for the thermal pulse to cross the annulus gap is

$$t_w = \frac{(1 - r_w)}{\frac{1}{\sqrt{Fo}}} = (1 - r_w)\sqrt{Fo} \tag{39}$$

Its corresponding dimensional time is

$$t_{w^*} = (r_{0^*} - r_{w^*})\sqrt{\tau_*/\alpha_*} \tag{40}$$

4. Analytical estimation of corrections to experimental data

When evaluating the thermal conductivity by applying the Transient Hot Wire method and using the Fourier Law one obtains from Eq. (18) the following solution for the dimensional temperature $T_{w^*}(t)$ at $r = r_w$

$$[T_{w^*}(t) - T_{C^*}] = \frac{q_{0^*} r_{o^*}}{k_{app}}[-r_w \ln(r_w) + f(t)] \tag{41}$$

where

$$f(t) = \sum_{n=0}^{\infty} C_n \exp\left[-\beta_n^2 t\right] \tag{42}$$

and for initial conditions of $T_o = 0$ the values of C_n are evaluated by using Eqs. (18) and (16). From Eq. (41) the thermal conductivity can be evaluated in the form

$$K_{act} = \frac{q_{o^*} L_*}{[T_{w^*}(t) - T_{C^*}]}[-r_w \ln(r_w) + f(t)] \tag{43}$$

where the temperature difference $[T_{w^*}(t) - T_{C^*}]$ is represented by the recorded experimental data and the value of the wall heat flux q_{0^*} is evaluated from the Joule heating of the hot wire in the form $q_{0^*} = iV/2\pi r_w l_*$, where $2\pi r_{w^*} l^*$ is the heat transfer area of the hot wire, with l^* being the length of the wire i is the electric current flowing through the wire and V is the voltage drop across the wire.

A method of *Synthetic Experimental Emulation Data* (*SEED*) is applied now to evaluate the deviation between Fourier and hyperbolic thermal conduction. According to the *SEED* method one assumes that the data expressed by $[T_{w^*}(t) - T_{C^*}]$ represent a different than the Fourier conduction solution, in this case a hyperbolic thermal conduction solution. Then the values of $T_{w^*}(t) - T_{C^*}$ were derived by using the hyperbolic solution presented in Eq. (27) evaluated at $r = r_w$ to yield

$$\frac{k_{app}}{k_{act}} = \frac{[-r_w \ln(r_w) + f(t)]}{[-r_w \ln(r_w) + h(t)]} \tag{44}$$

where k_{app} is the apparent thermal conductivity obtained from the Fourier conduction solution while k_{act} is the actual thermal conductivity that corresponds to data that follow the hyperbolic conduction, and where $f(t)$ can be evaluated from Eq. (42) while $h(t)$ is derived from the hyperbolic solution (27) evaluated at $r = r_w$. The ratio between the two will provide the deviation of the apparent thermal conductivity from the actual one.

5. Results and discussion

A comparison between the wire temperatures evaluated via Fourier and Hyperbolic solutions is presented in what follows. Fig. 2(a) shows the dimensionless wire temperature vs. dimensional time (on logarithmic scale) for copper in Ethylene Glycol using a combination of Dirichlet and Neumann boundary conditions for Fourier and Hyperbolic heat conduction problems with a Fourier number of $Fo = 10^{-3}$. Fig. 2(a) shows that for the time window of 10 s the Fourier heat conduction displays a linear result, and for the hyperbolic heat conduction the result looks almost linear. Only at times past 10 s the hyperbolic solution turns toward the Fourier solution and shows a non-linear curve. Therefore, when using the Transient Hot Wire method for a time window of up to 10 s to prevent convection a hyperbolic solution may seem linear and may be confused with the Fourier solution. Fig. 2(b) shows the dimensionless wire temperature vs. dimensional time (on logarithmic scale) for Carbon Nanotubes in Oil using a combination of Dirichlet and Neumann boundary conditions for Fourier and Hyperbolic heat conduction problems with Fourier number of $Fo = 10^{-3}$. This graph in Fig. 2(b) shows a similar result to the one in Fig. 2(a). For the time window of 10 s the hyperbolic heat conduction solution looks again almost linear and can be mistaken for the Fourier solution when using the Transient Hot Wire method.

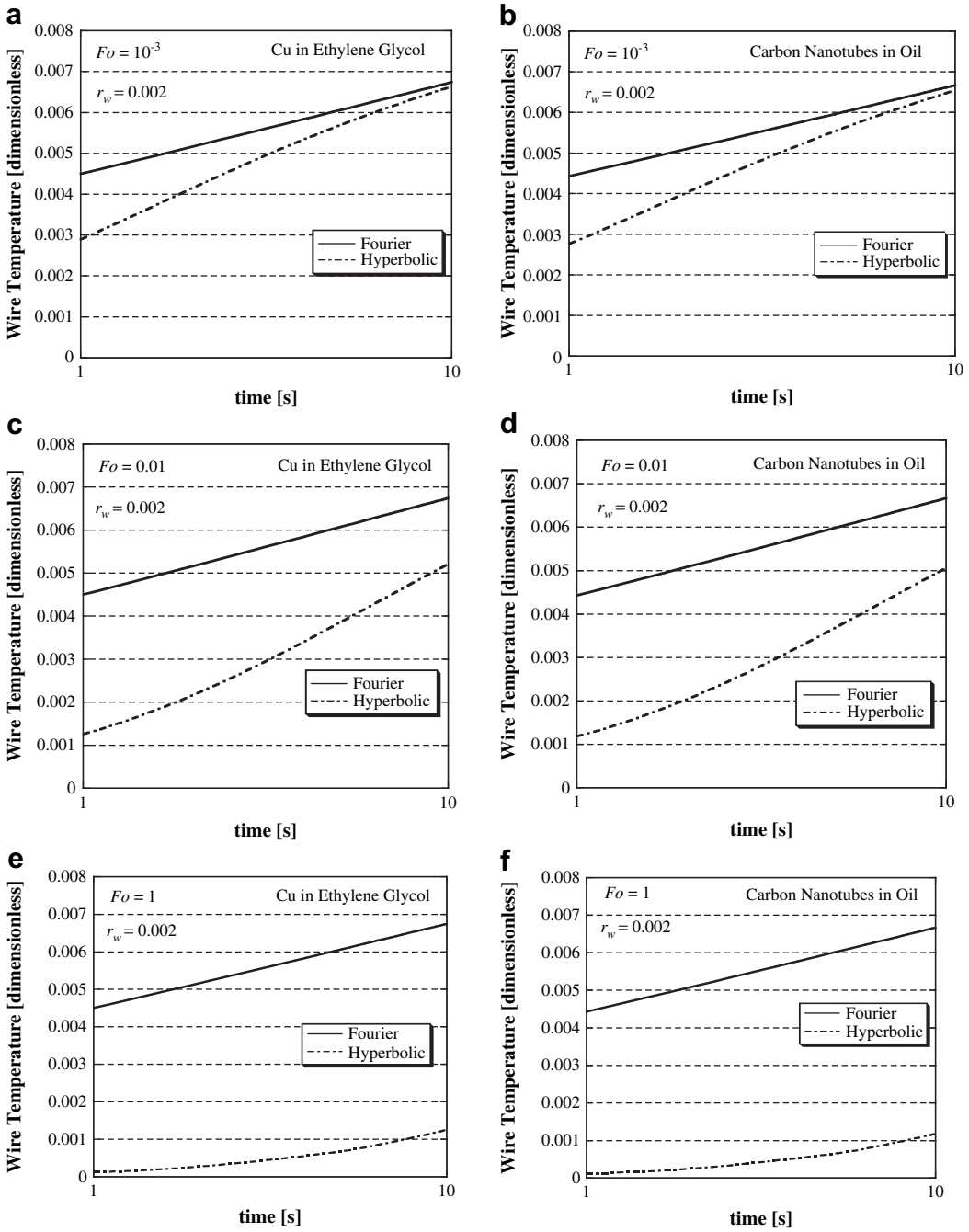

Fig. 2. The dimensionless wire temperature vs. dimensional time (on logarithmic scale) for copper in Ethylene Glycol (a, c, e) and Carbon Nanotubes in Oil (b, d, f) using a combination of Dirichlet and Neumann boundary conditions for Fourier and Hyperbolic heat conduction problems for different Fourier numbers.

Fig. 2(c) shows the dimensionless wire temperature vs. dimensional time (on logarithmic scale) for copper in Ethylene Glycol using a combination of Dirichlet and Neumann boundary conditions for Fourier and Hyperbolic heat conduction problems with Fourier number of $Fo = 0.01$. As the Fourier number is increased the wave effect becomes more apparent, however with a Fourier number of $Fo = 0.01$ the hyperbolic solution for the time window of 10 s still may pass for linear. For this reason it may be mistaken for the Fourier solution when using the Transient Hot Wire method. Fig. 2(d) shows the dimensionless wire temperature vs. dimensional time (on logarithmic scale) for Carbon Nanotubes in Oil using a combination of Dirichlet and Neumann boundary conditions for Fourier and Hyperbolic heat conduction problems with Fourier number of $Fo = 0.01$. From Fig. 2(d) one can draw the same conclusions as from Fig. 2(c). Fig. 2(e) shows the dimensionless wire temperature vs. dimensional time (on logarithmic scale) for copper in Ethylene Glycol using a combination of Dirichlet and Neumann boundary conditions for Fourier and Hyperbolic heat conduction problems with a Fourier number equal to 1 ($Fo = 1$). Fig. 2(f) shows the dimensionless wire temperature vs. dimensional time (on logarithmic scale) for Carbon Nanotubes in Oil using a combination of Dirichlet and Neumann boundary conditions for Fourier and Hyperbolic heat conduction problems with Fourier number equal to 1 ($Fo = 1$). Fig. 2(e) and (f) show that even when the Fourier number is 1 ($Fo = 1$), at a time window of 10 s the hyperbolic solution may still seem linear. This may be mistaken when using the Transient Hot Wire method for a Fourier solution.

The significance of the conclusions discussed above related to Fig. 2(a)–(f) is that when using the results obtained from the Transient Hot Wire method a Fourier solution is being used, even though a hyperbolic solution might be the one being revealed.

Generally, a hyperbolic thermal wave solution has the form of a sharp front of temperature moving from one boundary to the other at the propagation speed $c_* = \sqrt{\alpha_*/\tau_*}$. As a result, the same sharp front can be distinguished in plotting the temperature solution vs. time at any fixed spatial location. This sharp discontinuity is reflected in the results of the thermal conductivity ratio k_{app}/k_{act} obtained from the hyperbolic and Fourier solutions for a wide range of Fourier number values. These results were compared with the experimental data presented by Liu et al. [30] and are presented in Figs. 3–5. The thermal conductivity ratio results corresponding to Fourier number values of $Fo = 0.1$ and $Fo = 0.9$ are presented in Fig. 3. Fig. 4 shows the corresponding results for Fourier numbers of $Fo = 0.6$ and $Fo = 0.03$. The results for $Fo = 0.2$ and $Fo = 0.08$ are

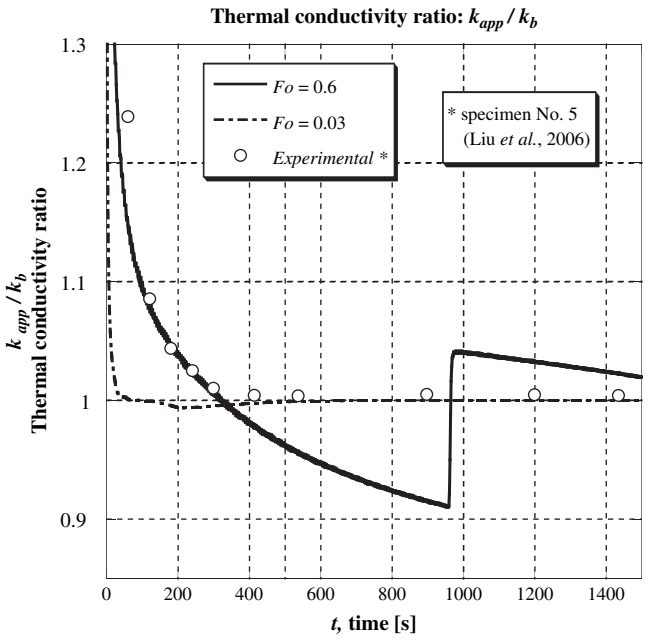

Fig. 4. Thermal conductivity ratio (k_{app}/k_{act}) from the hyperbolic solutions corresponding to properties of water and Fourier numbers of $Fo = 0.6$ and $Fo = 0.03$ compared to the experimental results from specimen 5 [30].

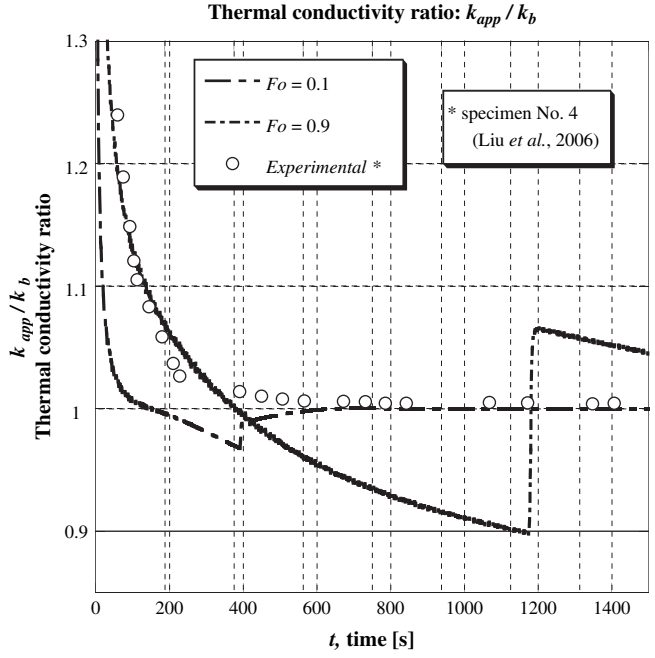

Fig. 3. Thermal conductivity ratio (k_{app}/k_{act}) from the hyperbolic solutions corresponding to properties of water and Fourier numbers of $Fo = 0.1$ and $Fo = 0.9$ compared to the experimental results from specimen 4 [30].

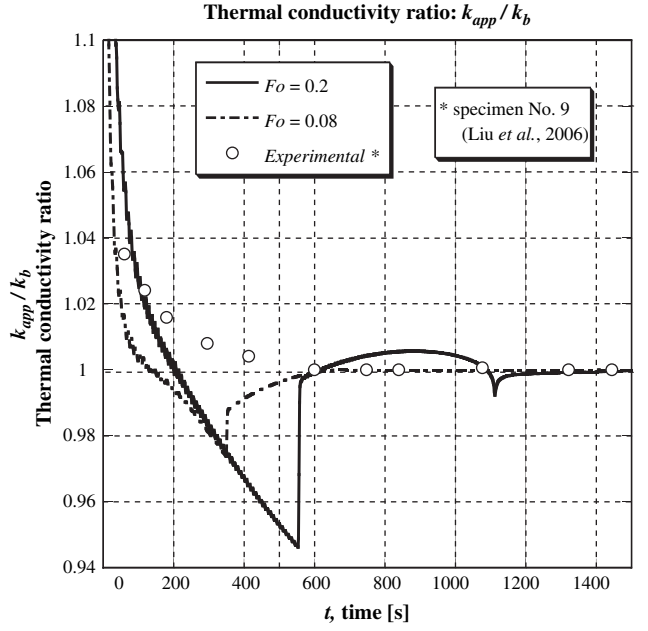

Fig. 5. Thermal conductivity ratio (k_{app}/k_{act}) from the hyperbolic solutions corresponding to properties of water and Fourier numbers of $Fo = 0.2$ and $Fo = 0.08$ compared to the experimental results from specimen 9 [30].

presented in Fig. 5. All three figures show that due to the sharp discontinuity in the hyperbolic solution which is revealed for not too small values of Fourier numbers there is no way to match the experimental data and therefore removing the hypothesis that thermal waves could have provided an explanation for the enhanced effective thermal conductivity in nanofluid suspensions.

6. Conclusions

The results obtained from this study suggest that the anticipation that thermal wave effects via hyperbolic heat conduction could have been the source of the excessively improved effective thermal conductivity of the suspension cannot be realized.

Acknowledgments

The authors wish to thank the National Research Foundation (NRF), the University of KZ-Natal, and the Department of Mechanical and Aeronautical Engineering at University of Pretoria, South Africa, for partially supporting this study.

Appendix. Supplementary data

Supplementary data associated with this article can be found, in the online version, at doi:10.1016/j.ijthermalsci.2009.06.002.

References

[1] S.U.S. Choi, Z.G. Zhang, W. Yu, F.E. Lockwood, E.A. Grulke, Anomalous thermal conductivity enhancement in nanotube suspensions, Appl. Phys. Lett. 79 (14) (2001) 2252–2254.
[2] J.A. Eastman, S.U.S. Choi, S. Li, W. Yu, L.J. Thompson, Anomalously increased effective thermal conductivities of ethylene glycol-based nanofluids containing copper nanoparticles, Appl. Phys. Lett. 78 (6) (2001) 718–720.
[3] W. Jiang, G. Ding, H. Peng, Measurement and model on thermal conductivities of carbon nanotube nanorefrigerants, Int. J. Therm. Sci., in press, doi:10.1016/j.ijthermalsci.2008.11.012.
[4] Y. Xuan, Q. Li, Heat transfer enhancement of nanofluids, Int. J. Heat Mass Transf. 21 (2000) 58–64.
[5] J.C. Maxwell, A Treatise on Electricity and Magnetism, third ed. Clarendon Press, Dover, New York, 1891, 1954 reprint, pp. 435–441.
[6] R.L. Hamilton, O.K. Crosser, Thermal conductivity of heterogeneous two-component systems, I&EC Fundam. 1 (1962) 187–191.
[7] D.J. Jeffrey, Conduction through a random suspension of spheres, Proc. R. Soc. London A 335 (1973) 355–367.
[8] R.H. Davis, The effective thermal conductivity of a composite material with spherical inclusions, Int. J. Thermophys. 7 (1986) 609–620.
[9] S. Lu, H. Lin, Effective conductivity of composites containing aligned spheroidal inclusions of finite conductivity, J. Appl. Phys. 79 (1996) 6761–6769.
[10] R.T. Bonnecaze, J.F. Brady, A method for determining the effective conductivity of dispersions of particles, Proc. R. Soc. London A 430 (1990) 285–313.
[11] R.T. Bonnecaze, J.F. Brady, The effective conductivity of random suspensions of spherical particles, Proc. R. Soc. London A 432 (1991) 445–465.
[12] S.A. Putnam, D.G. Cahill, P.V. Braun, Z. Ge, R.G. Shimmin, Thermal conductivity of nanoparticle suspensions, J. Appl. Phys. 99 (2006) 084308-1/6.
[13] R. Rusconi, E. Rodari, R. Piazza, Optical measurements of the thermal properties of nanofluids, Appl. Phys. Lett. 89 (2006) 261916-1/3.
[14] D.C. Venerus, M.S. Kabadi, S. Lee, V. Perez-Luna, Study of thermal transport in nanoparticle suspensions using forced Rayleigh scattering, J. Appl. Phys. 100 (2006) 094310-1/5.
[15] S. Lee, S.U.-S. Choi, S. Li, J.A. Eastman, Measuring thermal conductivity of fluids containing oxide nanoparticles, J. Heat Transf. 121 (1999) 280–289.
[16] B.X. Wang, L.P. Zhou, X.F. Peng, A fractal model for predicting the effective thermal conductivity of liquid with suspension of nanoparticles, Int. J. Heat Mass Transf. 46 (2003) 2655–2672.
[17] P. Keblinski, S.R. Phillpot, S.U.S. Choi, J.A. Eastman, Mechanisms of heat flow in suspensions of nano-sized particles (nanofluids), Int. J. Heat Mass Transf. 45 (2002) 855–863.
[18] J.A. Eastman, S.R. Philpot, S.U.S. Choi, P. Keblinski, Thermal transport in nanofluids, Annu. Rev. Mater. Res. 34 (2004) 219–246.
[19] R. Prasher, P. Bhattacharya, P.E. Phelan, Brownian-motion-based convective–conductive model for the effective thermal conductivity of nanofluids, J. Heat Transf. 128 (2006) 588–595.
[20] L. Xue, P. Keblinski, S.R. Phillpot, S.U.-S. Choi, J.A. Eastman, Effect of fluid layering at the liquid–solid interface on thermal transport, Int. J. Heat Mass Transf. 47 (2004) 4277–4284.
[21] P. Vadasz, Heat conduction in nanofluid suspensions, J. Heat Transf. 128 (2006) 465–477.
[22] M. Louge, X. Chen, Heat transfer enhancement in suspensions of agitated solids. Part HI: Thermophoretic transport of nanoparticles in the diffusion limit, Int. J. Heat Mass Transf. 51 (2008) 5130–5143.
[23] J. Vadasz, S. Govender, P. Vadasz, Heat transfer enhancement in nanofluid suspensions: possible mechanisms and explanations, Int. J. Heat Mass Transf. 48 (2005) 2673–2683.
[24] J. Kestin, W.A. Wakeham, A contribution to the theory of the transient hot-wire technique for thermal conductivity measurements, Physica 92A (1978) 102–116.
[25] R.A. Perkins, M.L.V. Ramires, C.A. Nieto de Castro, Thermal conductivity of saturated liquid toluene by use of anodized tantalum hot wires at high temperatures, J. Res. Natl. Instit. Stand. Technol. 105 (2000) 255–265.
[26] M.C. Cattaneo, Sur une forme de l'equation de la chaleur eliminant le paradoxe d'une propagation instantanee, C. R. Hebd. Seances Acad. Sci. 247 (4) (1958) 431–433.
[27] P. Vernotte, Les paradoxes de la theorie continue de l'equation de la chaleur, C. R. Hebd. Seances Acad. Sci. 246 (22) (1958) 3154–3155.
[28] P. Vernotte, La veritable equation de la chaleur, C. R. Hebd. Seances Acad. Sci. 247 (23) (1958) 2103–2105.
[29] P. Vernotte, Some possible complications in the phenomena of thermal conduction, C. R. Hebd. Seances Acad. Sci. 252 (1961) 2190–2191.
[30] Ming-Sheng Liu, M. Ching-Cheng Lin, C.Y. Tsai, Chi-Chuan Wang, Enhancement of thermal conductivity with Cu for nanofluids using chemical reduction method, Int. J. Heat Mass Transf. 49 (2006) 3028–3033.
[31] M.J. Assael, M. Dix, K. Gialou, L. Vozar, W.A. Wakeham, Application of the transient hot-wire technique to the measurement of the thermal conductivity of solids, Int. J. Thermophys. 23 (2002) 615–633.
[32] J.J. De Groot, J. Kestin, H. Sookiazian, Instrument to measure the thermal conductivity of gases, Physica 75 (1974) 454–482.
[33] J.J. Healy, J.J. de Groot, J. Kestin, The theory of the transient hot-wire method for measuring thermal conductivity, Physica 82C (1976) 392–408.
[34] J. Kestin, W.A. Wakeham, A contribution to the theory of the transient hot wire technique for thermal conductivity measurements, Physica 92A (1978) 102–116.
[35] U. Hammerschmidt, W. Sabuga, Transient hot wire (THW) method: uncertainty assessment, Int. J. Thermophys. 21 (2000) 1255–1278.
[36] Y. Nagasaka, A. Nagashima, Absolute measurement of the thermal conductivity of electrically conducting liquids by the transient hot-wire method, J. Phys. E: Sci. Instrum. 14 (1981) 1435–1440.
[37] M.J. Assael, K. Gialou, A transient hot wire instrument for the measurement of the thermal conductivity of solids up to 590 K, Int. J. Thermophys. 24 (2003) 667–674.
[38] M.J. Assael, K. Gialou, Measurement of thermal conductivity of stainless steel AISI 304L up to 590 K, Int. J. Thermophys. 24 (2003) 1145–1153.
[39] M.J. Assael, K. Gialou, K. Kakosimos, I. Metaxa, Thermal conductivity of reference solid materials, Int. J. Thermophys. 25 (2004) 397–408.
[40] M.J. Assael, K.D. Antoniadis, K. Kakosimos, I.N. Metaxa, An improved application of the transient hot-wire technique for the absolute accurate measurement of the thermal conductivity of Pyroceram 9606 up to 420 K, Int. J. Thermophys. 29 (2008) 445–456.
[41] J.J. de Groot, J. Kestin, H. Sookiazian, W.A. Wakeham, The thermal conductivity of four monatomic gases as a function of density near room temperature, Physica 92A (1978) 117–144.
[42] M.J. Assael, C.-F. Chen, I. Metaxa, W.A. Wakeham, Thermal conductivity of suspensions of carbon nanotubes in water, Int. J. Thermophys. 25 (2004) 971–985.
[43] M.J. Assael, I. Metaxa, J. Arvanitidis, D. Christofilos, C. Lioutas, Thermal conductivity enhancement in aqueous suspensions of carbon multi-walled and double-walled nanotubes in the presence of two different dispersants, Int. J. Thermophys. 26 (2005) 647–664.
[44] M.N. Ozisik, Heat Conduction, second ed. John Wiley & Sons, 1993.